

Development of All-Diamond Scanning Probes Based on Faraday Cage Angled Etching Techniques

C. Giese, P. Quellmalz and P. Knittel

Fraunhofer IAF, Fraunhofer Institute for Applied Solid State Physics, Freiburg/Germany

We are proposing a novel fabrication method for single crystal diamond scanning probes, exploiting the method of Faraday cage angled etching (FCAE). Electron-beam lithography (EBL) and inductively coupled plasma (ICP) etching as state-of-the-art method is often limiting the achievable diamond structure geometries in aspect ratio and complexity. This poses challenges, e.g., for realizing nitrogen vacancy (NV) centre magnetometry scanning probes. Combining a planar design with FCAE offers several advantages over the established fabrication technology of nano-opto-mechanical diamond devices. Here, we report on the direct comparison of both approaches and present first proof-of-concept FCAE-prototypes for scanning probe applications.

INTRODUCTION:

The outstanding properties of diamond such as extraordinary mechanical hardness, high thermal conductivity, wide bandgap, extremely broadband optical transparency or chemical inertness make it an interesting material for various application fields [1-3].

One of the latter are single crystal based scanning probes exhibiting excellent mechanical and optical properties [4].

The nitrogen Vacancy (NV) centre in diamond is the most studied and scientifically most promising among numerous diamond point defects for quantum communication, quantum computing and quantum sensing applications[5-9]. Combining scanning tips with single NV centres at the tip apex have paved the way for highly sensitive, quantitative sensing of magnetic fields on the nanometre scale[10-12].

Over the last decade a common fabrication method for NV-magnetometry scanning probes has been established[13,14] utilizing the thinning of nitrogen ion implanted commercially available diamond membranes down to single digit μm thickness. Consecutive EBL steps and plasma etching define the structure, geometry and size of opto-mechanical diamond devices. Using micromanipulators, the micron sized devices are removed from the membranes and attached to a mechanical spacer (millimetre length quartz fibres or silicon beams) which is in term fixed to a piezoelectric quartz tuning fork

on a printed circuit board (PCB) for use in a tuning-fork based atomic force microscopes (AFM).

Membrane based fabrication of diamond scanning probes is a challenging process that has therefore only been realized by few research teams over the world. We propose a new design of scanning tips based on Faraday cage angled etching (FCAE). The technique was developed in silicon semiconductor processing and first successfully applied to diamond in the Lončar group at Harvard university[15], especially focused on photonic applications [16,17]. In the following sections our progress on fabrication of membrane based as well as planar Faraday cage (see fig. 1) etched all-diamond devices will be presented and we will discuss the possible advantages of FCAE over the former approach.

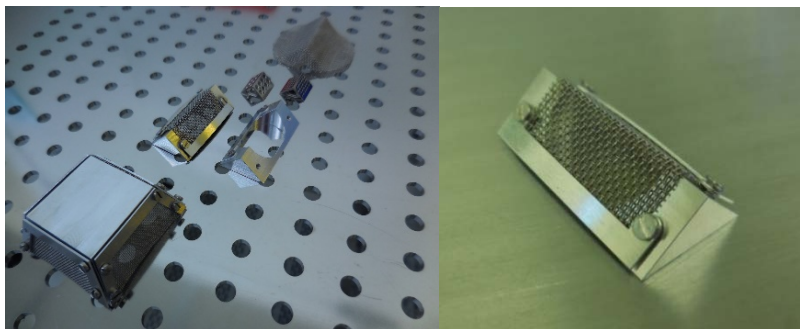


Fig.1: Left: Different Faraday cage designs (back to front): Formed stainless steel mesh (45° angle), nickel coated brass cage (45° angle), aluminium frame with clamped stainless steel mesh (45° angle), aluminium cage with stainless steel meshes for simultaneous etching from four directions (80° angle). **Right:** Close up of employed Faraday cage with 240 μm diameter wire mesh (740 μm pitch).

All-Diamond Device Fabrication

Membrane Based Vertical Diamond Devices

The fabrication process can be shortly summarized as follows. Thinned diamond plates are temporarily fixed to carrier substrates for processing and handling. An EBL defined etch process creates vertical waveguide structures simultaneously acting as AFM scanning tips. In a second lithography and dry etching step, the diamond devices are isolated, remaining attached to the membrane only via a thin beam that is ruptured during lift-out of the structures.

For device realization ultrapure, single crystalline (100)-oriented diamond substrates of 3x3 mm² size and 300 μm thickness were acquired (Element6 electronic grade CVD) as well as grown in proprietary-designed diamond microwave plasma enhanced chemical vapor deposition (MWPECVD) reactors. Details of the ellipsoidal micro-wave resonator design have been published elsewhere[18]. The bulk material was characterized via micro-photoluminescence ($\mu\text{-PL}$) in order to verify NV concentration in the low ppb range. Micro Raman analysis was performed to assess the sp³ phase purity and crystal quality (Renishaw Invia). Subsequently the samples were laser cut and

thinned via scaife polishing to yield 30 μm thickness membranes (DDK, Delaware diamond Knives inc.). Before processing, the samples were cleaned in nitric acid at 250 °C for 120 minutes.

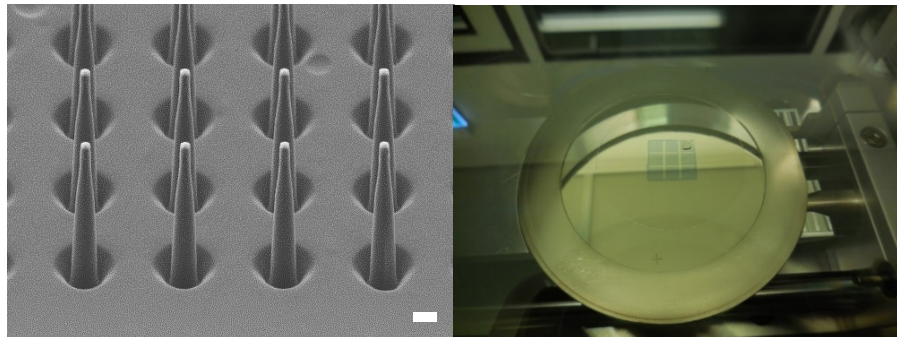


Fig.2: **Left:** SEM image of dry chemically oxygen etched vertical diamond waveguides (scale bar 500 nm). **Right:** Single crystalline diamond substrate on silicon carrier wafer in ICP etcher load lock chamber (Sentech SI500).

The implanted and annealed diamond plates were temporarily bonded to 3" silicon wafers (fig. 2) their implanted surface pointing upwards for cleanroom processing (HT10.10 bonding agent / Brewer Science, Süss SB6) which enables for easy handling and processing in semi-automatic tools. Due to its low sputter yield of 0.081 (100 eV argon ions) [19] titanium is a well suited mask material for diamond structuring. Selectivity of 100 and higher can be achieved for Oxygen based dry etching processes. In contrast to the most common approach, we therefore employed titanium metal masks enabling deep dry etching up to 50 μm , through the entire membrane.

The mask for vertical diamond waveguide structuring is defined via EBL (JBX9300FS, JEOL). A double layer of poly(methyl methacrylate) based resist (PMMA) is spin coated and e-beam exposure is performed. The PMMA is developed in a mixture of isopropanol and Methyl isobutyl ketone (MIBK) (3:1). Metal (75 nm Ti) is deposited via electron beam evaporation and lift-off in solvent removes the non-exposed resist. Vertical waveguides are structured via oxygen based inductively coupled plasma reactive ion etching (ICP-RIE / Sentech SI500). Etching parameters were as follows: 1.3 Pa chamber pressure, 700 W ICP power, 70 W RF platen power and 30 sccm oxygen flow. As shown in figure 2 high aspect ratio vertical waveguides with top diameters of 200 nm and bottom diameters of roughly 600 nm were formed. The typical etch depth is 3 μm at an etch rate of 200 nm/min.

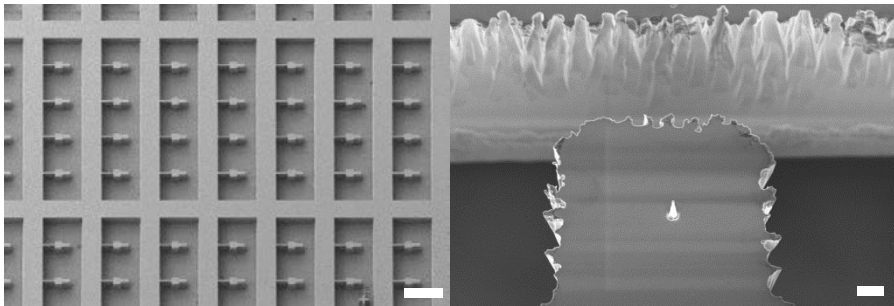


Fig.3: **Left:** SEM image of single crystalline membrane of 30 μm thickness with freestanding scanning probe tips (scale bar 100 μm). **Right:** Close up of vertical waveguide on isolated diamond device (scale bar 2 μm).

For backside lithography the diamonds are debonded and rebonded upside down on the carrier wafer after removal of the mask in hydrofluoric acid. Image reversal i-line mask aligner lithography (Süss MA6) was performed (AZ5214 resist, 1.4 μm thickness). Edge bead formation issues at distances of some hundred micrometres from the corners were avoided by designing a 400 μm frame enclosing all devices for mechanical stability after deep etching. Hard mask lift-off (100 nm Ti) was performed before RIE singulation of the cantilevers with dimensions of 20x40 μm^2 (fig. 3).

FCAE Based Planar Diamond Devices

For the novel device design the FCAE principle is shortly introduced. In low pressure reactive ion etching, a bias potential is formed between the neutral plasma and the cathode which holds the sample. This takes place when the light electrons follow the capacitively coupled RF field in the MHz range applied to the electrode, charging it negatively to up to several hundred volts. The bias field accelerates the heavier ions towards the cathode where they physically etch the target material. When a metallic Faraday cage is placed over the sample, the bias field follows the geometry of the cage and the impact angle of the ions is controlled by the inclination of the cage walls. Likewise, freestanding, triangular shaped diamond beams of complex geometry can be etched.

For prototype fabrication 4x4 mm electronic grade crystals (IIa HPHT, New diamond Technologies) of 500 μm thickness and (100) crystal orientation were wafer bonded as reported above. A 150 nm nickel mask was structured via EBL and lift-off. Different Faraday cages were designed and fabricated in order to assess the method (fig. 1). Tent-like aluminium frames with clamped meshes and sidewall angles of 45° were used in the presented work. The dimensions of the cage were 20x10x7 mm^3 , the mesh wire diameter was 240 μm and the pitch 740 μm .

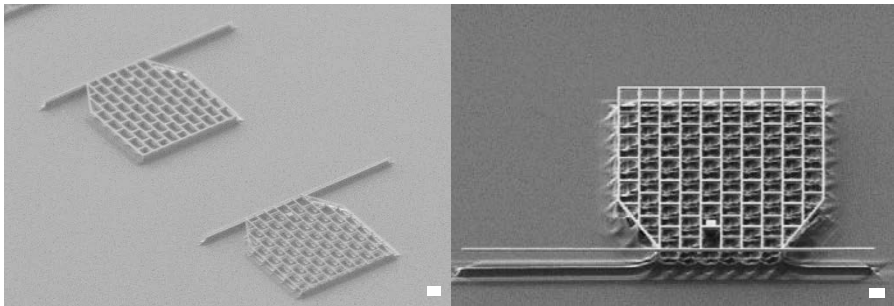


Fig.4: **Left:** Image of scanning probe structures with mechanical interface on the bulk diamond substrate (scale bar 3 μ m). **Right:** Close up of freestanding 50 μ m length beam (scale bar 2 μ m).

Faraday etching was performed placing the cage over the diamond sample on the carrier wafer and ICP parameters were slightly modified with respect to the vertical waveguide etch. For further enhancement of mask selectivity, RF platen power was reduced to 45 W, yielding a bias voltage of -100 V. As the cage design allowed for simultaneous etching from two directions, several etch steps were performed, switching between two orthogonal orientations of the faraday cage. SEM measurements confirmed complete underetching of the target structures after 22 min in each orientation. Lateral etch rate was estimated as 7-10 nm/min while vertical etch rate was 110 nm/min. The total etch depth of the finished devices was 4800 nm (fig. 4).

In order to enable the transfer of the devices, we define a fine grid as mechanical interface (fig. 4). A single beam attached to the grid acts as planar wave guiding structure allowing for high photon collections efficiency of NVs located at the extremity of the triangular beam simultaneously acting as AFM scanning tip.

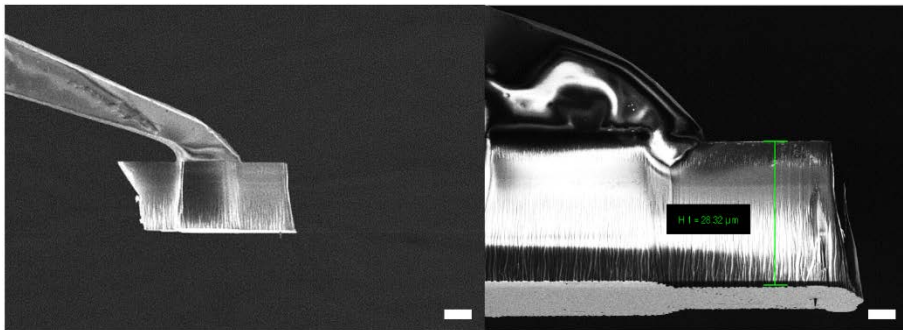


Fig.5: **Left:** SEM image of mounted SOI handle and diamond device (scale bar 10 μ m). **Right:** Close up of diamond device with 200 nm diameter vertical, conically shaped waveguide (scale bar 5 μ m).

Mounting of AFM Scanning Probes

In order to use micro-opto-mechanical diamond devices as AFM tips, they need to be mechanically interfaced with piezo-driven quartz tuning forks. For electrical contact and handling, the latter are fixed to custom PCBs with contact pads for drive and read-out control. For simultaneous scanning and optical read-out with high NA objectives quartz

fibres or SOI structures (fig. 5, left) with millimetre length are used as spacers to connect the tips to the tuning fork ($3 \times 1 \text{ mm}^2$).

The mounting of the membrane based, vertical (fig. 5) as well as the FCAE based, lateral micro-diamond devices (fig. 6) on the latter is achieved via micromanipulators (MiBot, Imina Technologies SA) and UV curing optical adhesive (NOA81, Norland).

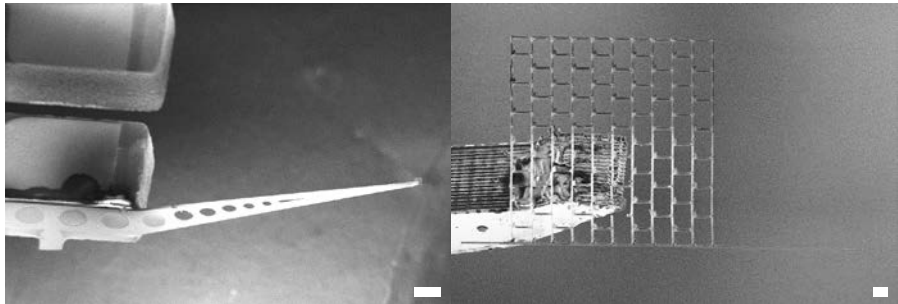


Fig.6: **Left:** SEM image of quartz tuning fork with mounted SOI handle and diamond device (scalebar 100 μm). **Right:** Mounted FCAE scanning probe tip with 300 nm width grid and triangular shaped waveguide (scalebar 2 μm).

Scanning Probe Characterization

The performance of the tuning fork scanning probes shown in figure 6 were investigated in a JPK Nanowizard III AFM system equipped with a tuning fork module. A tuning fork with a resonance frequency of approx. 32.75 kHz was chosen for the actuation of the diamond tip. Due to the attachment of the tip including the silicon handle, a decrease in resonance frequency of 0.5 kHz was measured.

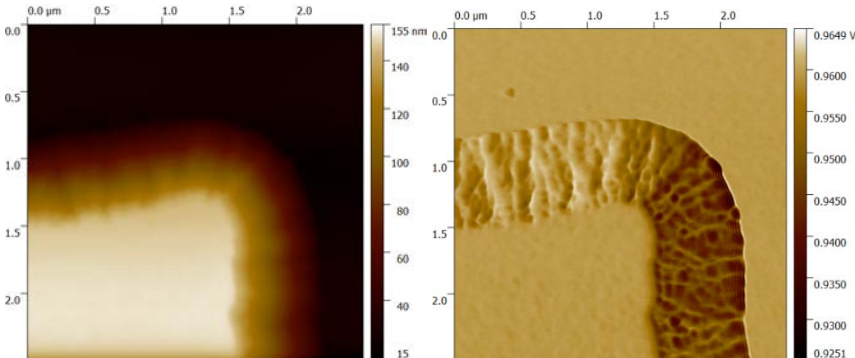


Fig.7: 2,5 μm^2 AFM scan of silicon oxide calibration sample with scanning probe prototype (5 nm pixel size). **Left:** height image of mesa sidewall. **Right:** Amplitude signal showing high resolution features of silicon oxide structure.

The ultra-high aspect ratio of the produced tip (>60) is suited for scans of target structures with steep sidewalls which are inaccessible for standard pyramidal silicon AFM tips (54° side wall angle). Figure 7 shows height and amplitude signals of a SiO_x calibration standard mesa structure. Apart from the overall topography of the mesa that is precisely imaged, the geometry of the sidewalls is obtained with high resolution. Especially the amplitude signal clearly reveals the morphology of the sidewall resulting from the fabrication of the calibration standard.

Discussion

FCAE based scanning probe fabrication yields key advantages over membrane based technology. Using bulk diamond substrates surmounts the challenging and costly production of electronic grade membranes [20,21]. Additionally, reuse of the ultra-pure substrates is possible making maximum use of the volume material, largely lost in the case of membrane polishing. The method overcomes wedge issues relevant for membrane fabrication, enabling the processing of larger substrates. In the presented work more than 2000 devices could be placed on a single 4x4 mm diamond, further optimization possible. The advantages of FCAE based diamond structuring offer new possibilities for multiple application fields. The facile fabrication of high aspect ratio (HAR) AFM tips [22,23] is one of them, addressing issues in AFM studies of high-topography samples. Furthermore, the scalable technique for designing larger mechanical interface surfaces enable for automated assembly of all-diamond AFM tips employing state of the art pick-and-place bonder tools. Single crystalline diamond MEMS [24,25] and photonic structures like optical waveguides or resonators [26] also have large potential.

Conclusion and Outlook

The presented novel FCAE-based method for producing all-diamond scanning probes opens up new design and fabrication possibilities for micron scale opto-mechanical devices. Especially the application to the scalable production of NV scanning probes is of interest to the growing community involved in the field of quantitative nanometre scale magnetometry.

We thank Jan Rhensius and Christian Degen from ETH Zurich for supplying SOI structures for scanning probe mounting and fruitful discussions.

This work was in funded within the European H2020 framework “AsteriQs” no. 820394 and the Fraunhofer-Max-Planck Cooperation program “DIANMR” no. 600717.

References:

- [1] R. S. Balmer, J. R. Brandon, S. L. Clewes, H. K. Dhillon, J. M. Dodson, I. Friel, P. N. Inglis, T. D. Madgwick, M. L. Markham, T. P. Mollart, N. Perkins, G. A. Scarsbrook, D. J. Twitchen, A. J. Whitehead, J. J. Wilman, S. M. Woollard, *Journal of physics. Condensed matter an Institute of Physics journal* **2009**, 21, 364221.
- [2] S. Koizumi, C. Nebel, M. Nesladek, *Physics and Applications of CVD Diamond*, Wiley **2008**.
- [3] C. E. Nebel, in *Nanodiamonds Micro and Nano Technologies* (Ed.: J.-C. Arnault), Elsevier **2017**, p. 1.
- [4] I. Aharonovich, A. D. Greentree, S. Prawer, *Nature Photon* **2011**, 5, 397.
- [5] G. Balasubramanian, I. Y. Chan, R. Kolesov, M. Al-Hmoud, J. Tisler, C. Shin, C. Kim, A. Wojcik, P. R. Hemmer, A. Krueger, T. Hanke, A. Leitenstorfer, R. Bratschitsch, F. Jelezko, J. Wrachtrup, *Nature* **2008**, 455, 648.
- [6] G. Balasubramanian, P. Neumann, D. Twitchen, M. Markham, R. Kolesov, N. Mizuuchi, J. Isoya, J. Achard, J. Beck, J. Tissler, V. Jacques, P. R. Hemmer, F. Jelezko, J. Wrachtrup, *Nature materials* **2009**, 8, 383.
- [7] A. Gruber, *Science* **1997**, 276, 2012.
- [8] R. Hanson, D. D. Awschalom, *Nature* **2008**, 453, 1043.
- [9] I. Aharonovich, T. Babinec, in *Comprehensive hard materials: Volume 1-3: Hardmetals, ceramics, super hard materials* (Eds.: C. E. Nebel, D. Mari, L. LLanes, V. K. Sarin), Elsevier. Amsterdam, Waltham, Heidelberg **2014**, p. 469.
- [10] G. P. Berman, A. R. Bishop, B. M. Chernobrod, M. E. Hawley, G. W. Brown, V. I. Tsifrinovich, *J. Phys.: Conf. Ser.* **2006**, 38, 167.

- [11] C. L. Degen, *Appl. Phys. Lett.* **2008**, *92*, 243111.
- [12] J. R. Maze, P. L. Stanwix, J. S. Hodges, S. Hong, J. M. Taylor, P. Cappellaro, L. Jiang, M. V. G. Dutt, E. Togan, A. S. Zibrov, A. Yacoby, R. L. Walsworth, M. D. Lukin, *Nature* **2008**, *455*, 644.
- [13] P. Appel, E. Neu, M. Ganzhorn, A. Barfuss, M. Batzer, M. Gratz, A. Tschöpe, P. Maletinsky, *The Review of scientific instruments* **2016**, *87*, 63703.
- [14] P. Maletinsky, S. Hong, M. S. Grinolds, B. Hausmann, M. D. Lukin, R. L. Walsworth, M. Loncar, A. Yacoby, *Nature nanotechnology* **2012**, *7*, 320.
- [15] M. J. Burek, N. P. de Leon, B. J. Shields, B. J. M. Hausmann, Y. Chu, Q. Quan, A. S. Zibrov, H. Park, M. D. Lukin, M. Lončar, *Nano letters* **2012**, *12*, 6084.
- [16] M. J. Burek, Y. Chu, M. S. Z. Liddy, P. Patel, J. Rochman, S. Meesala, W. Hong, Q. Quan, M. D. Lukin, M. Lončar, *Nature communications* **2014**, *5*, 5718.
- [17] P. Latawiec, M. J. Burek, Y.-I. Sohn, M. Lončar, *Journal of Vacuum Science & Technology B, Nanotechnology and Microelectronics: Materials, Processing, Measurement, and Phenomena* **2016**, *34*, 41801.
- [18] C. J. Widmann, W. Müller-Sebert, N. Lang, C. E. Nebel, *Diamond and Related Materials* **2016**, *64*, 1.
- [19] K. Wasa, in *Handbook of Sputtering Technology*, Elsevier **2012**, p. 41.
- [20] Y. Tao, C. Degen, *Advanced materials (Deerfield Beach, Fla.)* **2013**, *25*, 3962.
- [21] M. Challier, S. Sonusen, A. Barfuss, D. Rohner, D. Riedel, J. Koelbl, M. Ganzhorn, P. Appel, P. Maletinsky, E. Neu, *Micromachines* **2018**, *9*, 148.
- [22] A. Savenko, I. Yildiz, D. H. Petersen, P. Böggild, M. Bartenwerfer, F. Krohs, M. Oliva, T. Harzendorf, *Nanotechnology* **2013**, *24*, 465701.
- [23] A. Yacoot, L. Koenders, *New J. Phys.* **2008**, *41*, 103001.
- [24] Y. Tao, J. M. Boss, B. A. Moores, C. L. Degen, *Nat Commun*, **5**, 1.
- [25] P. Ovartchayapong, L. M. A. Pascal, B. A. Myers, P. Lauria, A. C. Bleszynski Jayich, *Appl. Phys. Lett.* **2012**, *101*, 163505.
- [26] P. Rath, S. Khasminskaya, C. Nebel, C. Wild, W. H. P. Pernice, *Nature communications* **2013**, *4*, 1690.